ICASSP 2021 - 2021 IEEE International Conference on Acoustics, Speech and Signal Processing (ICASSP) | 978-1-7281-7605-5/20/$31.00 ©2021 IEEE | DOI: 10.1109/ICASSP39728.2021.9415114

AN EFFICIENT PAPER ANTI-COUNTERFEITING METHOD BASED ON MICROSTRUCTURE ORIENTATION ESTIMATION

Yuhao Sun[1,2], Xin Liao[1,], Jianfeng Liu[2,3]*

[1] College of Computer Science and Electronic Engineering, Hunan Univerity, Changsha 410082, China
[2] Southeast Digital Economic Development Institute, Quzhou 324000, China
[3] College of Information Engineering, China Jiliang University, Hangzhou 310018, China

ABSTRACT

Forgery of paper invoices and certificates negatively causes huge economic loss every year. In the molding process of paper, plant fibres inside will distribute randomly and form the unique microscopic surface. Accordingly, forensic researchers have presented many techniques to build its feature descriptor for paper anti-counterfeiting. Among those methods, normal vector field and reconstructed surface based on multi-view photos captured by mobile camera have indicated incredibly effectiveness and practicality. However, the inefficiency of existing models using mobile camera is the neck in real time detection scenarios. In this paper, we focus on the efficient microstructure orientation estimation of paper surface for authentication. To address this problem, we investigate the reflection characteristics of rough surface and quantify the light attenuation accurately. Then, we model the entire propagation path of light emitted by flash, and exploit single photo captured by mobile camera to reconstruct microscopic inclination based on beam energy loss. Reduction of required pictures significantly enhances forensics efficiency. Through comparison experiments, we demonstrate that our proposed method can be used for paper discrimination effectively with speedy feature extraction.

Index Terms— Paper anti-counterfeiting, mobile camera, microstructure orientation estimation, light attenuation, forensics efficiency.

1. INTRODUCTION

Even though electronic information industries develop rapidly today, traditional paper documents and packages still play vital parts in finance, government office and pharmaceutical field. However, advances in printing technology and image manipulation tools have made it significantly easier to create fakes without leaving any perceptible details than ever before. Maliciously forged documents and certificates lead to huge economy loss every year, hence this problem has attracted much attention of forensic researchers.

Unlike conventional anti-counterfeiting methods which have complex processing techniques or high production cost, such as bar code authentication [1] and fluorescence detection [2], twisting plant fibres along with paper forming process can be regarded as a unique and reliable fingerprint for anti-counterfeiting [3, 4]. Therefore, researchers focus on these intrinsic microscopic structure of surface and develop associated feature descriptor for paper authentication. Buchanan *et al.* [3] initially utilizes the diffuse scattering of focused laser to measure the fine structure of paper surface. Kauba *et al.* [5] regarded the authentication of drug package as a paper texture classification problem using SVM. Schraml *et al.* [6] further introduced open set recognition and extracted package texture from multi view images as combined features. Another feature descriptor named dense micro-block difference (DMD) [7] could also be applied for surface texture extraction at multiple scales and orientations. Toreini *et al.* [8] proposed a fingerprint encoded from translucent patterns when the light shines through the paper. And Guarnera *et al.* [9] used local binary pattern (LBP) as a new descriptor of aforementioned patterns. However, it's worth noting that what above methods exploit is only the appearance or derived features extracted at the image level, without reconstructing the microscopic structure of paper surface. The latter is actually the root of appearance diversity in different pixel positions.

With the assistance of scanner, subtraction of two images from opposite scanning directions was leveraged for estimation of 3-D surface texture under linear light source [4]. Wong *et al.* [10] presented physically unclonable functions (PUFs) in paper anti-counterfeiting and demonstrated the effect of extrinsically introduced rough features on discrimination performance. To make authentication more flexible, the normal vector field of paper surface was built based on multi-view photos captured by mobile cameras [11]. For reaching higher verification accuracy, Liu *et al.* [12] further quantified the ambient light and optical adjustment inside camera and leveraged dif-

This work is supported by National Natural Science Foundation of China (Nos. 61972142, 61772191), Hunan Provincial Natural Science Foundation of China (No. 2020JJ4212), Key Lab of Information Network Security, Ministry of Public Security (No. C20611), Quzhou Science and Technology Project (Nos. 2020K24, 2019K12).

*Corresponding author: Xin Liao, xinliao@hnu.edu.cn.

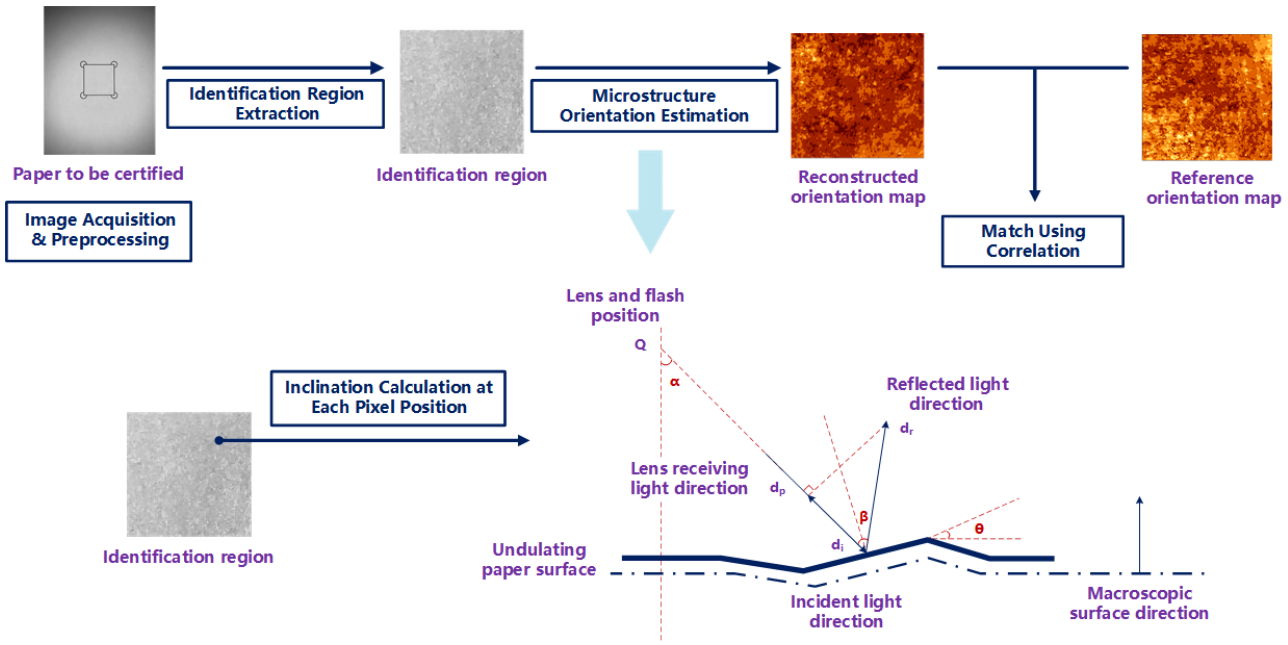

Fig. 1. Overall paper authentication framework based on microstructure orientation map of paper surface. And lower part of the figure indicates the complete propagation path of light, where θ expresses the inclination angle at pixel position p. In the optical path, when the light is incident at α, the angle between incident light direction d_i and reflected light direction d_r is denoted as β. Moreover, Q indicates the position of flash and lens, while d_p expresses the direction of lens receiving reflected light.

ference of gaussian (DoG) to separate frequency subbands of reconstructed surface .

Yet, the prerequisite of normal map and surface reconstruction is the detailed surface reflection information, which is usually estimated from multi-view pictures captured by high-definition image acquisition equipment. Consequently, their inefficiency on feature extraction will be the neck for actual application scenarios. In this paper, we transform the paper surface reconstruction into a microscopic inclination estimation problem. To begin with, we analyze the surface reflection characteristics and light attenuation to investigate the beam energy loss. According to the unique appearance at each pixel position, we reconstruct the microstructure orientation map. Precision metrics and time consuming are examined to demonstrate the effective performance of our method on discrimination accuracy and authentication efficiency.

2. PROPOSED METHOD FOR SURFACE MICROSTRUCTURE ORIENTATION ESTIMATION

In this section, we address paper anti-counterfeiting as a "paperprint" matching problem, which will be resolved by accurate estimation of microstructure orientation. Fig.1 depicts a general paper identification framework [11] we follows. In our case, the framework consists of four main components, which respectively are image acquisition and preprocessing, identification region extraction, microstructure orientation estimation and match using correlation. For the third component, in order to carefully describe the microtopography, we demonstrate the beam energy loss based on the diffuse reflection of rough surface and the light attenuation. Finally we reconstruct the surface microstructure orientation map for paper authentication. The remaining three components will be illustrated in section 3.

2.1. Reflection Characteristic of Rough Surface

Owing to the rough surface formed by twisting and undulating fibres inside, our proposed method is according to the diffuse reflection principle. Moreover, unique distribution of fibres leads to different appearances when the paper is illuminated by changing incident light. In a shooting environment with flash on [11] to weaken ambient interference, the beam reaching on each pixel position contains not only the ambient light, but also the part emitted by flash. In most cases, the intensity and relative direction of flash dominate the appearance of pixels because of its more powerful energy and closer distance. Just like mountains and valleys under the sunlight, the raised part of microscopic paper surface will reflect light back to the lens, while the sunken part will nearly not. Therefore, when the light source changes its location relative to the paper surface, "mountains" with different inclinations will present distinct appearances. That's to say, diversity of pixel values will be specified by these differences of appearance.

2.2. Quantification of Beam Energy Loss

In this part, we model the complete propagation path of light as shown in lower part of Fig.1. Then, we use $\mathbb{L}_{Emi}$ and $\mathbb{L}_{Rbk}$ to denote the amount of photons emitted by flash and reflected back to lens respectively. Besides, $\mathbb{L}_{Wst}$ indicates the wastage of energy. According to the reflection characteristic demonstrated in section 2.1, we propose the definition of the beam energy loss:

Definition 1 *In a complete light propagation process, total loss of beam energy can be expressed as:*

$$\mathbb{L}_{Wst} = \mathbb{L}_{Emi} - \mathbb{L}_{Rbk} \tag{1}$$

However, $\mathbb{L}_{Emi}$ is difficult to quantify in reality, thus we have to infer another form of $\mathbb{L}_{Wst}$. Specifically, we assume that the flash is a point light source which is different from the parallel ambient light. Hence, when the light emitted by flash passes through the air, it follows the negative quadratic power decay law. Noted that the attenuation continues throughout the entire propagation path of light, and this is consistent with real physical scenes.

In general, if we use $\mathbb{L}_{Att}$ and $\mathbb{L}_{Dif}$ to indicate the wastage caused by light attenuation and photons which are not reflected back to the lens respectively, the variant form of beam energy loss can be defined as:

Definition 2 *Total wastage of beam energy can be denoted as the sum of attenuation loss and reflection loss, i.e.,*

$$\mathbb{L}_{Wst} = \mathbb{L}_{Att} + \mathbb{L}_{Dif} \tag{2}$$

Recall the reflection characteristic introduced in section 2.1, different values at each pixel position stem from their unique microtopography. Meanwhile, diverse heights and inclinations will lead to different energy loss. Therefore, it's possible to deduce the microstructure orientation map inversely.

2.3. Optical Path and Orientation Map Estimation

In order to realize the authentication, we need to reconstruct the microstructure orientation map following by Definition 2 demonstrated in section 2.2. To do this, the beam energy in each part of optical path needs to be counted. Following the negative quadratic decay law, $\mathbb{L}_{Att}$ is quantified as the initial light intensity divided by the square of propagation distance. Accordingly, light intensity that each pixel position p receives can be denoted as:

$$l_{rev}(p) = \frac{\sum_{i=1}^{k} v(p_i) \cdot d(p_i)^4}{k \cdot d(p)^2} \tag{3}$$

where k is total number of pixels in the identification region, $v(p)$ expresses the real pixel value, and $d(p)$ indicates distance between lens position Q and pixel position p.

Accordingly, the real pixel value can be derived jointly by $l_{rev}(p)$ and the energy loss $l_{dif}(p)$ introduced by diffuse reflection as follows:

$$v(p) = \frac{l_{rev}(p) - l_{dif}(p)}{d(p)^2} \tag{4}$$

Substituting Eq.(3) into Eq.(4), we can infer $\mathbb{L}_{Dif}$ at each pixel position p as $l_{dif}(p)$ that:

$$l_{dif}(p) = \frac{\sum_{i=1}^{k} v(p_i) \cdot d(p_i)^4}{k \cdot d(p)^2} - v(p) \cdot d(p)^2 \tag{5}$$

On the basis of angle relationship illustrated in Fig.1, we can deduce that:

$$\beta = \arccos(1 - \frac{l_{dif}(p)}{l_{rev}(p)}) \tag{6}$$

and finally obtain the microscopic inclination θ at pixel position p as:

$$\theta = \arccos(\frac{h(Q)}{d(p)}) - \frac{1}{2}\arccos(\frac{k \cdot v(p) \cdot d(p)^4}{\sum_{i=1}^{k} v(p_i) \cdot d(p_i)^4}) \tag{7}$$

where $h(Q)$ expresses the vertical distance between lens and the horizon plane.

After traversing each pixel position in identification region, all inclinations together form the orientation map which can be used for the further matching. For more intuitive, we visualize the map as Fig.2 (a). The brighter regions inside indicate microscopic surfaces with a bigger inclination towards lens, while the darker parts are on the contrary. Our proposed method does not involve complex matrix calculations and minimum number of photos required, so as to achieve speedy forensics.

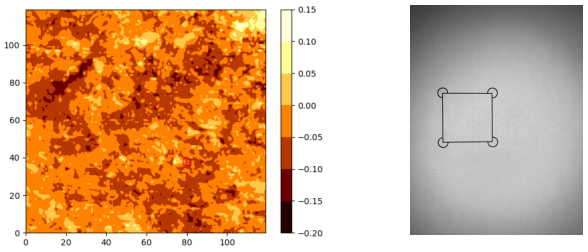

(a) Orientation map (b) Identification region

Fig. 2. Identification region in paper surface and its corresponding microstructure orientation map. (a) Top view of reconstructed orientation map, where the colorbar illustrates the relative inclination at each pixel position with radian as unit. (b) Example of registration container and identification region inside.

3. EXPERIMENTAL RESULTS

In this section, we show the performance comparison between our method and existing models on discrimination accuracy and efficiency.

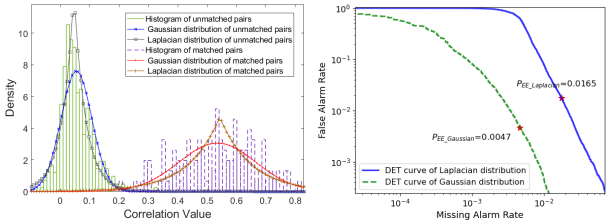

(a) Frequency distribution (b) DET curve with EER

Fig. 3. The frequency histogram of correlation values and detection error tradeoff curve of the fitted distribution. (a) Histograms and fitted Gaussian and Laplace distribution corresponding to unmatched cases (H_0) and matched cases (H_1) respectively. (b) DET curves of Gaussian and Laplace fitting distribution with their equal error rate.

3.1. Dataset and Experimental Setup

For dataset acquisition, photos are taken from seven different A4 printing paper sheets. Moreover, we introduce the registration container from [10] with square identification region inside as shown in Fig.2 (b). To simulate the changing ambient light in actual scenarios, we take shots in the morning, dusk and night respectively with the flash of mobile phone on. Besides, contrast limited adaptive histogram equalization (CLAHE) [13] is applied to improve the local contrast of image and suppress the noise amplification during the pixel mapping. Then, we exploit hough and perspective transformation to extract the identification region for the further orientation map reconstruction. Our machine configuration for experiment is Intel(R) Core(TM) i7-9700F CPU @ 3.00GHz with 16.0 GB RAM and the edition of Python and Matlab is 3.6 and R2017b respectively.

3.2. Correlation Matching Using Orientation Map

In order to evaluate discrimination performance of our proposed method, we introduce the hypothesis testing framework from [11, 14]. The null hypothesis H_0 is that the identification region to be verified does not match the reference, while the alternative hypothesis H_1 is the match situation. Pearson correlation coefficient [15] is used as a test statistic to quantify the degree of correlation between the test and reference surfaces. Fig.3 (a) intuitively presents that the unmatched cases are concentrated in the left with correlation values around 0.05, while the values of matched cases are around 0.55 in the right side.

In addition, we apply Gaussian and Laplace distribution to fit the frequency distribution of correlation values under selected thresholds. They can reveal the upper and lower bound of classification capability respectively [11]. As shown in Fig.3 (b), false alarm and missing alarm rate are examined to express the detection error tradeoff (DET) curve and equal error rate (EER) of the two fitting functions, which indicate the discrimination performance of proposed method.

Table 1. Comparison of discriminative performance among our proposed method, normal map [11] and the highest frequency subband [12].

Methods	EER	AP	AUC	d-prime
Normal map (4 pics) [11]	0.4581	0.6175	0.5745	0.7919
Subband #1 (4 pics) [12]	0.2247	0.8542	0.8290	0.4447
Normal map (8 pics) [11]	0.0188	**0.9999**	**0.9999**	0.9094
Subband #1 (8 pics) [12]	0.1216	0.9351	0.9807	0.5501
Proposed method	**0.0165**	0.9989	0.9996	**1.3477**

Table 2. Comparison of feature extraction efficiency among our proposed method, normal map [11] and the highest frequency subband [12].

Methods	Images required	Total processing time	
Normal map [11]	≥ 4	$39.81s$ (4 pics)	$76.35s$ (8 pics)
Subband #1 [12]	≥ 4	$28.77s$ (4 pics)	$40.73s$ (8 pics)
Proposed method	**1**	**$2.81s$**	

3.3. Comparing with Existing Models

In this subsection, we investigate the performance on discrimination and efficiency of the proposed method and existing models [11, 12] . Note that the two models for comparison are based on the photo captured by mobile phones as well.

In the comparison experiment, 4 images are minimum demand for the estimation of normal map [11] and surface reconstruction [12]. Table 1 examines the common classification performance metrics, such as average precision (AP), area under the ROC curve (AUC) and EER of heavy-tail Laplacian distribution. Experimental results indicate that when reconstructed using 8 photos, the discrimination performance of normal map will approach to the proposed method. However, Table 2 expresses that the authentication efficiency of our work is approximately 27 times better than it. we additionally introduce the d-prime [16] index to compare classification performance between low error rate systems. As shown in Table 1, the proposed method could improve the d-prime by 48.2% comparing with Normal map (8 pics) case.

4. CONCLUSION

In this paper, we proposed the microscopic orientation map of paper surface to achieve efficient and accurate paper authentication. We analyzed the reflection characteristic of rough surface, quantified the beam energy loss throughout the whole optical path and finally estimated the microscopic inclination of paper surface. Comparative experiments prove the effectiveness of our proposed method. In future work, we will further refine the model granularity and test the possible affect of paper materials, external printing/handwriting and so on.

5. REFERENCES

[1] H. P. Nguyen, F. Retraint, F. Morain-Nicolier and A. Delahaies, A watermarking technique to secure printed matrix barcode—application for anti-counterfeit packaging, *IEEE Access*, 2019, pp. 131839-131850.

[2] H. Guo, B. Yin, J. Zhang, Y. Quan and G. Shi, Forensic classification of counterfeit banknote paper by x-ray fluorescence and multivariate statistical methods, *Forensic Science International*, 2016, pp. e43-e47.

[3] J. D. R. Buchanan, R. P. Cowburn, A. V. Jausovec, *et al.*, Forgery: 'fingerprinting' documents and packaging, *Nature*, 2005, 436(7050), p. 475.

[4] W. Clarkson, T. Weyrich, A. Finkelstein, N. Heninger and E. W. Felten, Fingerprinting blank paper using commodity scanners, *30th IEEE Symposium on Security and Privacy*, 2009, pp. 301-314.

[5] C. Kauba, L. Debiasi, R. Schraml and A. Uhl, Towards drug counterfeit detection using package paperboard classification, *Pacific Rim Conference on Multimedia*, 2016, pp. 136-146.

[6] R. Schraml, L. Debiasi, C. Kauba and A. Uhl, On the feasibility of classification-based product package authentication, *IEEE Workshop on Information Forensics and Security (WIFS)*, 2017, pp. 1-6.

[7] R. Mehta and K. Egiazarian, Texture classification using dense micro-block difference, *IEEE Transactions on Image Processing*, 2016, pp. 1604-1616.

[8] E. Toreini, S. F. Shahandashti and F. Hao, Texture to the rescue: Practical paper fingerprinting based on texture patterns, *ACM Transactions on Privacy and Security (TOPS)*, 2017, 20(3), pp. 1-29.

[9] F. Guarnera, D. Allegra, O. Giudice, F. Stanco and S. Battiato, A new study on wood fibers textures: Documents authentication through LBP fingerprint, *IEEE International Conference on Image Processing (ICIP)*, 2019, pp. 4594-4598.

[10] C. W. Wong and M. Wu, A study on PUF characteristics for counterfeit detection, *IEEE International Conference on Image Processing (ICIP)*, 2015, pp. 1643-1647.

[11] C. W. Wong and M. Wu, Counterfeit detection based on unclonable feature of paper using mobile camera, *IEEE Transactions on Information Forensics and Security*, 2017, 12(8), pp. 1885-1899.

[12] R. Liu, C. W. Wong and M. Wu, Enhanced geometric reflection models for paper surface based authentication, *IEEE International Workshop on Information Forensics and Security (WIFS)*, 2018, pp. 1-7.

[13] K. Zuiderveld, Contrast limited adaptive histogram equalization, *Graphics Gems*, 1994, pp. 474-485.

[14] B. C. Levy, Principles of signal detection and parameter estimation, *Springer Science and Business Media*, 2008.

[15] J. Benesty, J. Chen, Y. Huang and I. Cohen, Pearson correlation coefficient, *Noise Reduction in Speech Processing*, 2009, pp. 1-4.

[16] E. Eban, M. Schain, A. Mackey, A. Gordon, R. Rifkin and G. Elidan, Scalable learning of non-decomposable objectives, *Artificial Intelligence and Statistics*, 2017, pp. 832-840.